Indian Journal of Biochemistry & Biophysics
Vol. 60, October 2023, pp. 770-778
DOI: 10.56042/ijbb.v60i10.397

Fabrication of phyco-functionalized zinc oxide nanoparticles and their *in vitro* evaluation against bacteria and cancer cell line

Geethalakshmi Ramakrishnan[1], Sirajunnisa Abdul Razack[1,2], Logeswari Ravi[1] & Renganathan Sahadevan[1]*

[1]Centre of Biotechnology, Alagappa College of Technology, Anna University, Chennai-600 025, Tamil Nadu, India

[2]Marine Integrated Biomedical Technology Center, The National Key Research Institutes in Universities, Pukyong National University, Busan 48513, Republic of Korea

Received 08 April 2023; *revised 12 August 2023*

Macroalgae with innumerable metabolites are predominantly identified as potential organisms in industrial and pharmaceutical applications. Herein, an attempt was made to fabricate zinc oxide nanoparticles (ZnO NPs) using the aqueous extract of red macroalgae *Kappaphycus alvarezii* and evaluate its anti-tumor and anti-bacterial activities, *in vitro*. ZnO NPs was prepared via chemical reduction (C-ZnO NPs), for comparative analysis, and co-precipitation method with the extract (B-ZnO NPs). Chemical composition analyses, physical characterization by UV Spectrophotometer, Fourier Transform InfraRed (FTIR) spectroscopy, Energy Dispersive X-Ray Analysis (EDX) and Scanning Electron Microscopy (SEM) and anti-oxidant ability by DPPH assay were performed. Anti-microbial activity of the fabricated nanomaterials was performed against *E. coli, Bacillus subtilis* and *Staphylococcus aureus*. Cell toxicity study was carried out using MTT assay upon 3T3 and MCF-7 cell lines. The study resulted that the presence of phenolic content in the algal extract enhanced the biological activities of ZnO NPs at an optimized concentration of 100 mM. Total phenolic content was exa mined to be 83.73 mg gallic acid eq/g and the maximum efficiency of DPPH scavenging was revealed by the concentration of 51.99 mg/mL. Anti-bacterial effect of B-ZnO NPs demonstrated maximum efficiency at the concentrations of 800 µg/mL, 400 µg/mL and 600 µg/mL against *Escherichia coli, Bacillus subtilis* and *Staphylococcus aureus* respectively. The cell viability study denoted that the fabricated B-ZnO NPs were non-toxic towards 3T3 while significant cytotoxicity was observed against MCF-7 at an IC_{50} of 75 µg/mL at 48 h. In conclusion, the B-ZnO NPs was observed to be effective as both bactericidal and anti-cancerous nano-agent and considered further for pharmaceutical applications.

Keywords: Antineoplastic, Bactericide, Co-precipitation, *Kappaphycus alvarezii,* Nano-agent

Metal NPs have been investigated as biological agents and as novel therapeutic agent carriers against various disorders. They are synthesized via physical, chemical and biological approaches. Albeit, physical and chemical methods give a voluminous yield, the use of laborious equipments and toxic chemicals as reducing, stabilizers and capping agents, a method of replacements is expected. Biological preparation of NPs is generally considered non-toxic due to the involvement of natural resources and their high surface to volume ratio which aid in creating better contact with bacteria to eventually cause bacterial lysis[1,2]. The biocidal effect has led such biological NPs to be utilized in drug delivery, environmental bioremediation, anti-microbial and cancer treatment[2].

In general, the physical properties of ZnO NPs lead to blocking of UV radiations. In comparison to other metallic nanoparticles, it stands out for its exceptional biocompatibility, tunable band gap, cell selectivity, stability, and good reducing nature[3]. Biologically generated zinc oxide nanoparticles (B-ZnO NPs) possess distinctive crystalline structure, high durability, thermal resistance, and high surface to volume ratio. It has been reported that lethality of cancer cells is caused by ZnO NPs through DNA damage and apoptosis, which are mediated by oxidative stress without harming healthy cells[4]. Numerous studies have demonstrated that ZnO NPs exhibited selective cytotoxicity against cancer cells and eliminate malignant cells through the interpretation of selective localisation and cell cytotoxicity[1].

Macro algae serve as a remarkable source in various biological applications out of which its implementation in nanomaterial synthesis has drawn attention in recent years. This is due to the fact that the macroalgae are found to be a reservoir of several secondary metabolites that could act as reducing and capping agents of synthesized nanoparticles and do not require any additional toxic chemicals as in chemical synthesis. *Kappaphycus alvarezii* is a marine red alga with high

*Correspondence:
E-mail: srenganathan@annauniv.edu

economic value due to the phycocolloids known as carrageenan on its cell walls[5]. The variants of this alga are red, brown, yellow and green based on the pigments produced by the seaweed[6]. The red strain is rich in carbohydrates, proteins, calcium, iron, vita min C and various bioactive compounds providing it nutraceutical and therapeutic properties[7,8]. The secondary metabolites such as phycoerythrin, fucoxanthin, maraniol or methyl coumarin and saponins are reported to be efficient against several cancers including colon, leukemia, adenocarcinoma and breast[5,9].

In this present investigation, B-ZnO NPs were synthesized using the aqueous extract of *K. alvarezii.* The B-ZnO NPs were assessed for their biological activities namely anti-bacterial and anti-tumorigenic and the effects were compared with the chemically synthesized ZnO NPs (C-ZnO NPs).To best of our knowledge, no study evaluating B-ZnO NPs against MCF-7 breast cancer cell lines has been reported.

Materials and Methods

Collection of Macroalga

*Kappaphycus alvarezii*was collected from the coastline regions of Ramanathapuram, Tamil Nadu, India which is considered to be one of the nation's hot spot areas of marine biodiversity.

Extraction of *K. alvarezii*

The algal sample was washed twice with sterile distilled water in order to remove debris and then washed with 70% ethanol. The cleaned samples were then placed in hot air oven (100°C for 5 h) which was then collected, blended into powder, sieved and stored for further experimentation. Solvent extraction was carried out by mixing the powdered alga in distilled water in the ratio of 1:10 at room temperature (RT) of 29°C. The mixture was left without agitation for 5 min in order to avoid swelling of the particles and then centrifuged at 3000 rpm for 15 min. The supernatant was collected and stored at 18°C until further analysis.

Analysis of the algal extract

Phytochemical analysis of the algal extract was carried out by Harborne method to identify the presence or absence of secondary metabolites[10].

Total phenolic content of the extract was determined using Folin-Ciocalteau reagent method. Gallic acid was taken as the standard. To 15 µL of crude solvent extract, 75 µL of folin-ciocalteau reagent and 60 µL sodium carbonate were added. The mixture was incubated for 30 min in dark. The absorbance was read at 765 nm. The value obtained was expressed in µg of gallic acid per gram of sample[4].

To determine the flavonoid content, to a volume of 10 µL sample, 4 µL of 5% $NaNO_2$ was added and incubated for 6 min at RT. Then, to the incubated sample, 4 µL of 10% $AlCl_3$ and 40 µL of 4% NaOH were added and the solution was made up to 100 µL with 100% ethanol. The mixture was incubated at RT for 15 min and the absorbance of the incubated sample was read at 510 nm against the standard, quercetin[11].

The anti-oxidant activity of the crude aqueous extract was determined using DPPH assay with Vitamin C as the standard. To 125 µL of sample, 50 µL of DPPH was added and incubated at dark for 30 min at RT. The absorbance was read at 518 nm[12].

Chemical and biological syntheses of ZnO NPs

For chemical synthesis, to 0.1 M zinc sulphate heptahydrate solution, 0.4 M NaOH was added drop wise at a ratio of 1:10. For biological synthesis, aqueous algal extract was mixed with 0.1 M zinc sulphate heptahydrate solution at a ratio of 1:10. In both cases the reaction was performed to eventually observe white and pale red precipitation as the C-ZnO NPs and B- ZnO NPs, respectively, visually. The solutions were adjusted to basic pH (pH 11) and stored overnight in dark. Then, the solutions were centrifuged at 3000 rpm for 20 min and, washed twice with distilled water and once with absolute ethanol. The resulting pellets were dried in hot air oven and powdered using mortar and pestle to finally obtain C-ZnO NPs and B-ZnO NPs.The samples were stored at 18°C until further analysis.

Characterisation of C- and B- ZnO NPs

The formation of C- and B-ZnO NPs was validated using a UV-visible spectrophotometer (G10S, Thermo Fisher Scientific Ltd., USA) by scanning the sample at wavelength ranging between 300 and 700 nm. The structural properties were determined by FTIR spectroscopy with wave number ranging between 4000 and 400 cm^{-1} (JASCO 6300, Japan) to denote the functional groups in the nanoparticles aiding as capping and reducing agents. Scanning Electron Microscope (SEM) equipped with Energy dispersive X-ray system (EDAX) (Jeol, Japan) was used to analyse the morphology and presence of elemental zinc in the fabricated materials, respectively[13].

Anti-bacterial assessment of C- and B-ZnO NPs

Bactericidal ability of the C- and B-ZnO NPs against different microorganisms were examined using agar well diffusion method. The cultures namely *Escherichia coli, Bacillus subtilis* and *Staphylococcus aureus* were subcultured into a sterile nutrient broth and incubated at 37±2°C for 24 h. Each culture was then transferred to

two batches of sterile nutrient agar plates through swabbing technique. For agar diffusion method, wells of 4 mm diameter were punched using a gel puncher. To each well of each batch, varying concentrations of C- and B-ZnO NPs (200, 400, 600, 800 and 1000 µg/mL) were added and kept for incubation at 37±2°C for 24 h. After incubation, the zone was measured (mm) against ampicillin (15 µg/mL) as the standard[14].

***In vitro* cytotoxicity**

Preparation of cell culture

Healthy fibroblast cell line, 3T3, and breast cancer cell line, MCF 7, were cultured in Dulbecco's modified Eagle's medium (DMEM) supplemented with 10% FBS. The medium was supplemented with 100 U/mL of penicillin, 100 µg/mL streptomycin and 2 mmol/L glutamine. Cell culture was cultivated and maintained in a humidified incubator with 5% CO_2 at 37°C for 24 and 48 h, respectively. Each cell line was authenticated and regularly tested for mycoplasma contamination[15].

Cytotoxicity assay

The cells were seeded in 96-well plates at a density of 5,000 cells per well. After an overnight incubation, cells were treated with different concentrations of C- and B-ZnO NPs for 24 and 48 h. Cell viability was measured using MTT assay according to the manufacturer's instruction (Sigma-Aldrich). The absorbance was assessed and denoted as optical density by reading the samples at 520 nm using a microplate reader(BioTek, USA, Synergy H1)[15].

Results and Discussion

Analysis of the algal extract

The algal extract was obtained from dried powder of the seaweed by using distilled water as the solvent (Fig. 1). In the aqueous algal extract, major secondary metabolites namely flavonoids, saponins and phenols were evinced. Most of the phytoconstituents reside in the polar solvents because of the dielectric constant that corresponds to the polarity of the solvents[3].These phytochemicals play a vital role in reducing the precursors to elemental or oxide forms of the nanoparticles and also simultaneously cap them during synthesis. Phenols and flavonoids act as anti-microbial and anti-cancer agents by disrupting the cell membrane and interfere with RNA, DNA, proteins and other cellular components[16]. They are also reported to be effective anti-oxidants, responsible for anti-microbial and anti-cancer properties. The highest phenolic and flavonoid contents were observed to be 83.734 mg GAE/100 g dry weight (DW) and 23.550 mg/g DW. This study corroborated with earlier reports. The phenolic content of *Kappaphycus* species cultivated in Malaysia was observed to be 7.51±0.16 to 19.17±0.04 mg GAE/g DW[17]. Total phenolic content of brazil farmed seaweed varied with the climatic conditions. At summer, it was observed to be 46.26±112.52 mg GAE/g DW while at autumn, it was 101.39±24.73 mg GAE/g DW[7]. The anti-oxidant ability was investigated of the fabricated nanomaterials which revealed an effective scavenging activity. Maximum radical scavenging activity was observed in water extract with concentration of 51.99 mg/g B-ZnO NPs. Presence of ascorbic acid, vitamin A, phenols and carrageenan, a sulfated polysaccharide on their cell wall, might have contributed to its anti-oxidant capacity[18].

Synthesis of C- and B-ZnO NPs

For the preparation of ZnO NPs, zinc sulphate was used as the precursor at different molar concentrations of 0.001 M, 0.01 M, 0.05 M and 0.1 M (Fig. 2A). Among them, 0.1 M resulted in the highest yield (0.5 g/100 mL). During chemical synthesis, cloudy white precipitate was obtained and centrifuged to finally result in C-ZnO NPs. In biological synthesis (B-ZnO NPs), to the precursor seaweed solution to reduce and functionalise the nanoparticles (Fig. 2B). The nanoparticle synthesis was noted by pale red precipitate formation. Generally,

Fig. 1 — Image demonstrating wet *Kappaphycus alvarezii* being dried and phytochemicals being extracted by solvent extraction method

electrochromism-based visual expression of colour shift was the initial proof of NPs formation. Due to the free neutral hydroxyl ion present on the surface, ZnO NPs exhibit an unusual electrostatic behaviour that allows any targeted proteins or chemical compounds to adhere, resulting in the selective killing of tumours[3]. Similar to the present study, ZnO NPs synthesized using *Ulva fasciata delile* was observed by color change and resulted good anti-bacterial effect[19]. Additionally, ZnO NPs synthesized using aqueous extract of red seaweed *Pterocladia capillacea* exhibited effective water treatment by adsorbing ISMATE violet 2R ions[20].

Characterization of C- and B-ZnO NPs

Ultraviolet Visible (UV-Vis) Spectroscopy

The absorbance of C-and B-ZnO NPs was read by scanning using a UV-Vis spectrophotometer ranging between 300-700 nm in order to examine surface plasmon resonance. The maximum wavelength obtained for C-ZnO NPs and B-ZnO NPs were noted as 370 nm and 360 nm, respectively (Fig. 3A). The electromagnetic

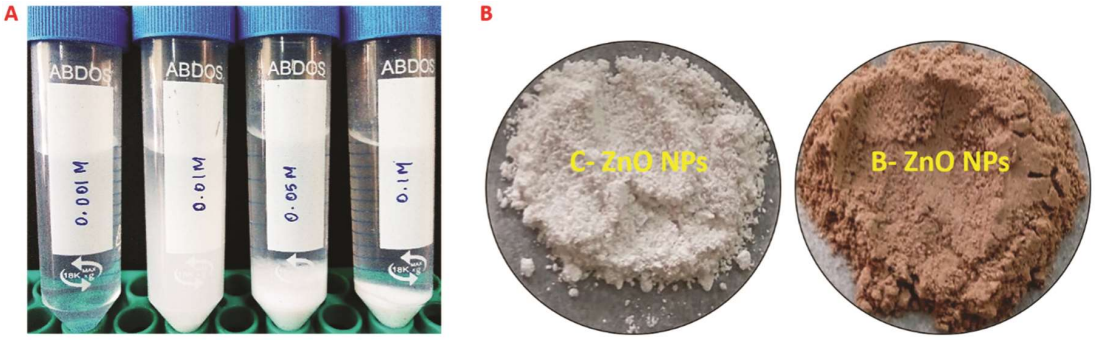

Fig. 2 — (A) Image illustrating the concentration optimization of C-ZnO NPs; and (B) final synthesized products (C- and B-ZnO NPs)

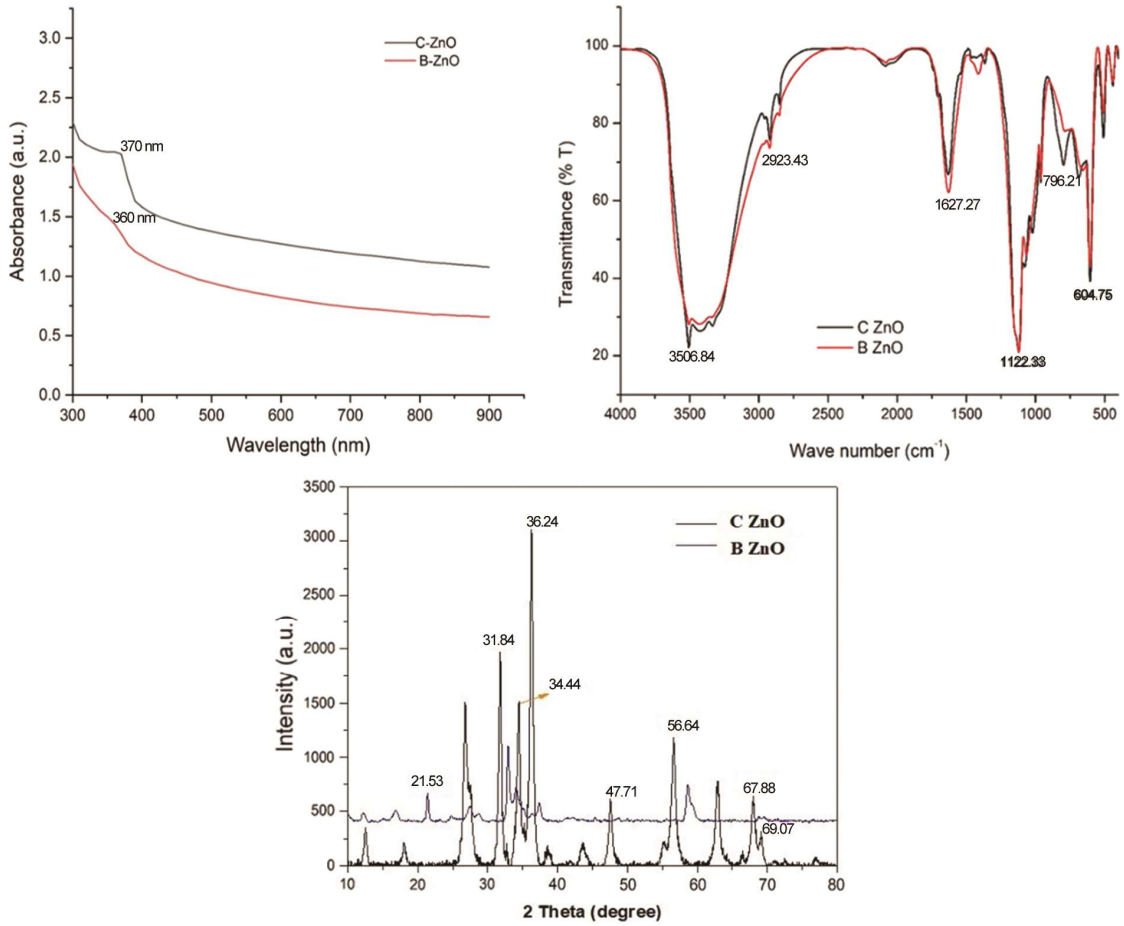

Fig. 3 — (A) UV-Vis spectral graphs, (B) FTIR spectra; and (C) XRD diffractograms of C- and B-ZnO NPs

forces that drove the surface excitation of electrons resulted in surface plasma resonance[3]. The present results agreed with previously studied reports. The peak observed at 315 to 400 nm resulted in the characteristic presence of Zn[21]. A peak at 377 nm was observed for ZnO NPs synthesized using *Turbinaria ornate*[22]. *Sargassum muticum* mediated synthesis of ZnO NPs resulted in an UV-Vis absorption peak at 350 nm[23].

Fourier Transform Infra Red Spectroscopy

FTIR spectroscopy is utilised to evaluate the organic molecules that contributes to the bioactive substances present in the analytes. The oscillation or breaking of the bonds caused by over excitation causes the peaks as shown in Fig. 3B and enables the transmission of IR radiation in the wave number ranging between 4000 and 500 cm^{-1}. For C-ZnO NPs, the major peaks were found to be at 3506.84 cm^{-1}, 2923.43 cm^{-1}, 1627.27.33 cm^{-1}, 1122.33 cm^{-1}, 796.21 cm^{-1} and 604.74 cm^{-1}. The band intensity of polar groups was represented at 3779-3002 cm^{-1} corresponding to hydroxyl group (O-H stretching), 1770-1639 cm^{-1} and, 796.21 cm^{-1} corresponded to alkene (C=C). The peak 1122.33 cm^{-1} was linked to strong C-O secondary alcohol[24]. The presence of bioactive substances like flavonoids and phenols (B-ZnO NPs), responsible for the bioconversion of ZnO NPs, was observed by shortening or shifting of peaks indicating the capping of ZnO NPs by the biomolecules. The intense stretching in the spectrum, 604 cm^{-1}, confirmed the presence of zinc oxide nanoparticles.

X Ray Diffraction analysis

The XRD pattern of ZnO NPs illustrated the characteristic peaks at 31.84°, 34.44°, 36.24°, 47.71°, 56.64°, 67.88°, 69.07° corresponding to the lattice planes (100), (002), (101), (110), (103), (112), (201)[25]. The peak shift in XRD was related to the structural changes in the nanoparticles. The peak at 21.53° corresponded to the presence of *K. alvarezii*[26] (Fig. 3C). These peaks are similar to the standard JCPDS PDF no. 36-1451 for ZnO NPs[27].

Surface morphology

Surface of the ZnO NPs were found to be well defined nanoflakes that revealed larger lateral dimensions in micrometer[28]. B-ZnO NPs were reduced in size when compared to C-ZnO NPs (Fig. 4A and B). The size of the nanoparticles was found to be less than 100 nm at a magnification of 200k X. The collective formation of nanoflakes was due to the electrostatic interactions between the extract and Zn^{2+} ions[29]. The elementsZn and O present in the nanoparticles which attributed to the ZnO NPs formation were determined using EDAX[30]. The

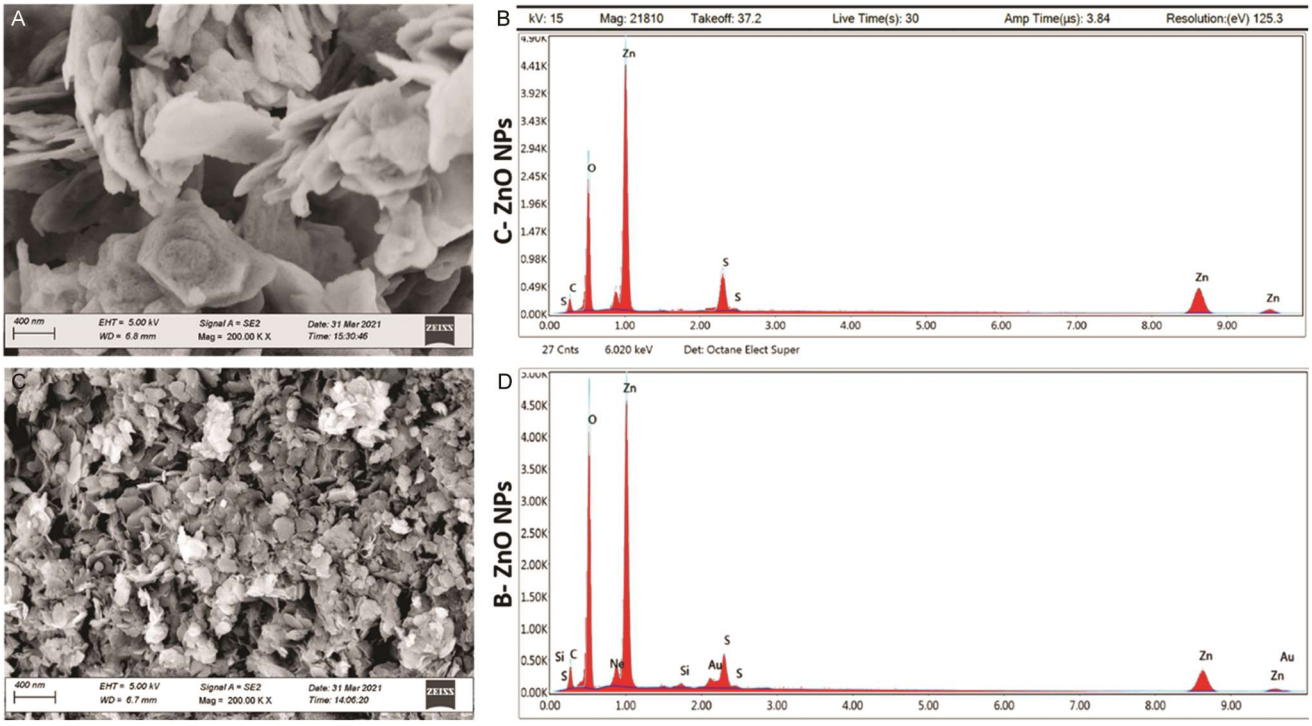

Fig. 4 — SEM images of (A) C- and (B) B-ZnO NPs and, EDAX spectra of (C) C- and (D) B-ZnO NPs

weight percentage of metallic zinc, oxygen, carbon present in C- and B-ZnO NPs were found to be 56.52, 25.58, 9.72 and 49.67, 32.1, 9.79, respectively (Fig. 4C and D). Similarly, in the ZnO NPs produced by *S. marginatum* and *U. lactuca*, Zn and O were (51.6 and 48.4%) and (48.3 and 51.7%), respectively[31]. The weight percentages of Zn and O in the ZnO NPs produced with the aqueous extract of *Nostoc* sp. were 31.8 and 63.2%, respectively[32].

Anti-microbial activity

The overall experimental results of C- and B-ZnO NPs exhibited good anti-bacterial activity and efficient inhibition against *E. coli, B. subtilis* and *S. aureus* was observed at concentrations of 800, 400 and 600 µg/mL, respectively, (Table 1). The mechanism behind the activity is due to the generation of reactive oxygen species (ROS). On the surface of ZnO particles, electron and hydrogen ions engage in a series of redox reactions with oxygen and water to produce ROS with high chemical activity[33]. The release of Zn^{2+} ions from ZnO NPs, which interact with negatively charged cells, may also be responsible for their anti-bacterial effects. Similar to the current study, ZnO NPs using red paprika (*Capsicum annuum* L. var. grossum (L.) Sendt)[34] and *Dictyota dichotoma* showed significant anti-microbial activity[35]. The impact of zinc oxide nanoparticles adsorbed on synthetic neodymium, revealed distinct anti-bacterial action against *E. coli* that produced extended-spectrum-lactamases (ESBLs)[36]. The green synthesised ZnO NPs at a concentration of 10 mg/mL exhibited anti-microbial activity[37]. The highest zone of inhibition of ZnO NPs synthesized using *Pterolobium hexapetalum* leaves extract was exhibited at 50 µg/mL against *E. coli*[38].

Cytotoxicity studies

MTT assay was carried out with five different concentrations (5, 10, 20, 25, 50 and 100 µg/mL) for 24 and 48 h to determine the cytotoxic effect of C- and B-ZnO NPs on 3T3 and MCF 7 cell lines. The untreated cells were used as control. The assay showed that, in comparison to the control, treatment of 3T3 cells and MCF-7 with increasing amounts of activity of C- and B-ZnO NPs led to cell death and suppression of cell viability (Fig. 5A and B). The cytotoxicity of nanoparticles against 3T3 has no significant effect upto the concentration 100 µg/mL which indicated the C- and B-ZnO NPs was highly biocompatible as nanocarriers. The IC_{50} value for C- and B-ZnO NPs in MCF-7 was found to be 100 µg/mL. The cytotoxicity data revealed that the treated groups exhibit an increased level of cell death. It can be hypothesised that when cells are treated with C- and B-ZnO NPs, there will be an accumulation of Zn^{2+} in the cytosol and the bioactive compounds of the extract released into the cytosol, will result in an increased production of free radicals and oxidative stress and possibly cause DNA and cell membrane damage as well as loss of cellular function. Further, the released bioactive substances trigger apoptotic signals, which cause cell death[39]. The phenylboronic acid (PBA) conjugated ZnO NPs resulted a LC_{50} value at 33.06 µg/mL[40]. ZnO NPs was identified to exhibit efficient anti-cancer activity due to its ROS generation which leads to cancer cell death[33]. When employed to deliver and load hydrophobic anti-cancer medicines, ZnO NPs exhibit remarkable behaviour due to its low toxicity that is studied using 3T3 fibroblast cells. It revealed that the cell growth inhibition was observed in MCF-7 by increasing the concentration of nanoparticles.Many reported studies have shown that zinc oxide nanoparticles are highly selective and highly cytotoxic to a variety of cell lines such as MCF-7, Caco-2, HepG2, A549, HT-29 and BEAS-2B, but show no toxic effects on normal cells[41]. The copper/zinc bimetallic NPs exhibited toxic effect at the concentration of 600 µg/mL[42]. The IC_{50} value of conjugated Nu-ZnO NPs was found to be 46 µg/mL[43].

Table 1 — Anti-microbial activity of ZnO NPs at varying concentration against different microorganisms

Culture	Drug concentration (µg/mL)										
	15	200		400		600		800		1000	
	Std	C-ZnO	B-ZnO	C-ZnO	B-ZnO	C-ZnO	B-ZnO	C-ZnO	B-ZnO	C-ZnO	B-ZnO
	Zone of inhibition (mm)										
E. coli	30±0.26	9±0.19	11±0.06	10±0.11	13±0.02	12±0.21	15±0.13	15±0.21	18±0.05	15±0.16	18±0.09
B. subtilis	24±0.03	10±0.05	11±0.24	11±0.09	13±0.15	11±0.10	13±0.16	11±0.11	13±0.18	11±0.18	13±0.19
S. aureus	28±0.23	10±0.09	13±0.23	12±0.11	16±0.14	15±0.26	18±0.29	15±0.27	18±0.30	15±0.28	18±0.31

Values expressed as mean ± SD

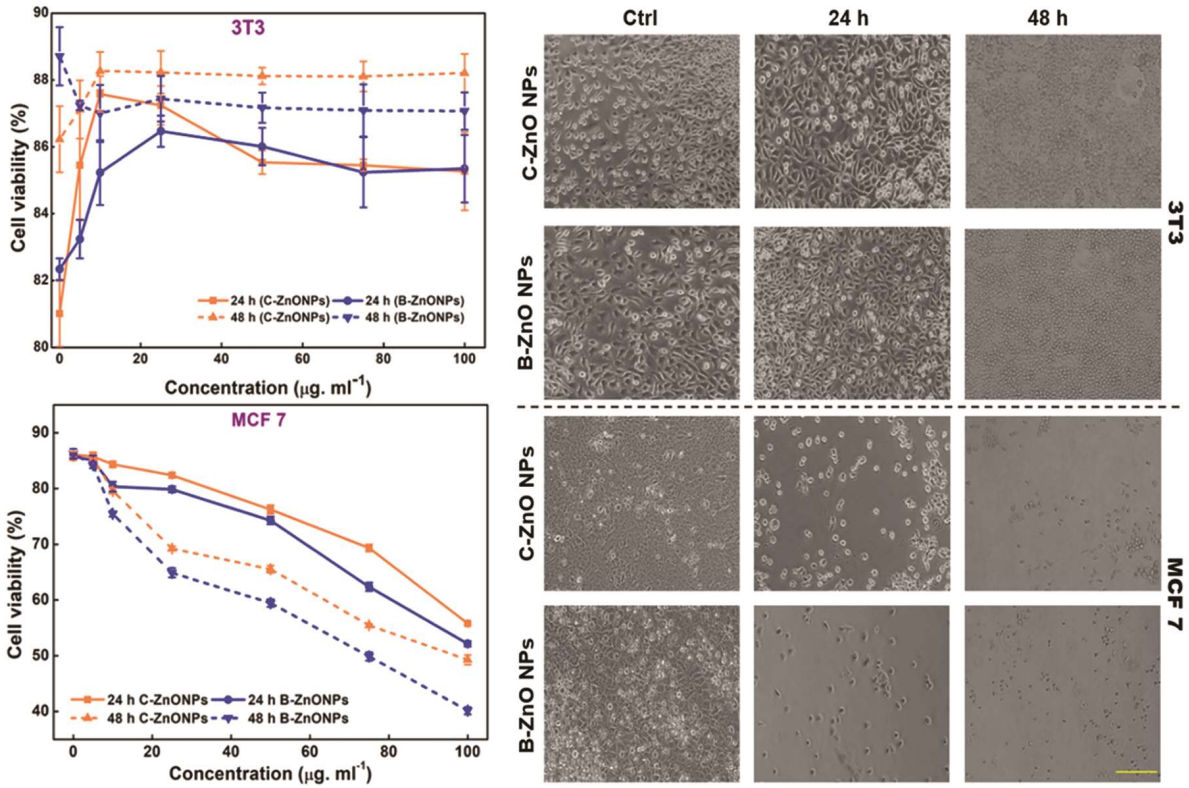

Fig. 5 — Cell viability assay for (A) 3T3; (B) MCF-7 cell lines; and (C) microscopic images of tested drugs at regular time intervals (10 X magnification; scale bar – 200 µM)

Conclusion

A simple, inexpensive, environmentally friendly and facile method was reported to form phyco-functionalized ZnO NPs (B-ZnO NPs) using aqueous seaweed extract. It was shown that the aqueous *K. alverazii* extract can be used as both a reducing agent and a protective agent for preparing the B-ZnO NPs. The as prepared C-and B-ZnO NPs were nanoflakes in structure whichwas confirmed by SEM analysis. The XRD patterns and EDAX demonstrated the crystallinity and purity of the B-ZnO NPs fabricated using a biogenic, greener approach. The toxicity of C- and B-ZnO NPs was tested by MTT assay on 3T3 and MCF-7 cell lines to exhibit effective anti-tumor activity. They conferred MCF-7 cytotoxicity by regulating proliferation and inducing apoptosis. C- and B-ZnO NPs were also successful in bacterial lysis. Consequently, these findings demonstrated the capability to synthesise ZnO NPs using *K. alverazii* aqueous extract using an upfront, one-pot, environmentally friendly method and its novel anti-breast cancer activity *in vitro* that may open up a novel stage for biomedical applications.

Acknowledgement

The authors thank the Department of Biotechnology, Anna University for providing the laboratory to carry out the extensive research work.

References

1 Alaizeri ZM, Alhadlaq HA, Aldawood S, Akhtar MJ & Ahamed M, One-pot synthesis of SnO2-rGO nanocomposite for enhanced photocatalytic and anticancer activity. *Polym*, 14 (2022) 2036.

2 Chau TP, Brindhadevi K, Krishnan R, Alyousef MA, Almoallim HS, Whangchai N & Pikulkaew S, A novel synthesis, analysis and evaluation of Musa coccinea based zero valent iron nanoparticles for antimicrobial and antioxidant. *Environ Res*, 209 (2022) 112770.

3 Chelladurai M, Sahadevan R, Margavelu G, Vijayakumar S, González-Sánchez ZI & Vijayan K, Anti-skin cancer activity of *Alpinia calcarata*ZnO nanoparticles: Characterization and potential antimicrobial effects. *J Drug Deliv Sci Technol*, 61 (2021) 102180.

4 Chelladurai M, Margavelu G, Vijayakumar S, González-Sánchez ZI, Vijayan K & Sahadevan R, Preparation and characterization of a mine-functionalized mupirocin-loaded zinc oxide nanoparticles: A potent drug delivery agent in targeting human epidermoid carcinoma (A431) cells. *J Drug Deliv Sci Technol*, 70(2022) 103244.

5 Kothai R, Arul B & Anbazhagan V, Anti-dengue activity of ZnO nanoparticles of crude fucoidan from brown seaweed S. marginatum. *Appl Biochem Biotechnol*, 195 (2023) 3747.

6 Adharini RI, Setyawan AR & Jayanti AD, Comparison of nutritional composition in red and green strains of *Kappaphycus alvarezii* cultivated in Gorontalo Province, Indonesia. *E3S Web Conf*, 147 (2020) 03029.

7 Araújo PG, Nardelli AE, Duran R, Pereira MS, Gelli VC, Mandalka A, Eisner P, Fujii MT & Chow F, Seasonal variation of nutritional and antioxidant properties of different *Kappaphycus alvarezii* strains (Rhodophyta) farmed in Brazil. *J Appl Phycol*, 34(2022)1677.

8 Vaghela P, Das AK, Trivedi K, Anand KV, Shinde P & Ghosh A, Characterization and metabolomics profiling of *Kappaphycus alvarezii* seaweed extract. *Algal Res*, 66 (2022) 102774.

9 Dewi NP, Santoso J, Setyaningsih I &Hardingtyas SD, Extraction of phycoerythrin from *Kappaphycus alvarezii* seaweed using ultrasonication. *IOP Conf Ser Earth Environ Sci*, 414 (2020) 012028.

10 Khan MS, Ranjani S & Hemalatha S, Synthesis and characterization of *Kappaphycus alvarezii* derived silver nanoparticles and determination of antibacterial activity. *Mater Chem Phys*, 282 (2022) 125985.

11 Karuppannan S, Govindasamy B, Lakshmanan A, Maluventhan V & Arumugam M, Bioactive compounds of Marine Red algae Portieria hornemannii and its bio control effects against Culex quinquefasciatus dengue vectors. *J Pharm Negat Results*, 1 (2022) 1128.

12 Wang X, Feng Z, Li C, Cai X, Long H, Zhang X, Huang A, Zeng Y, Ren W & Xie Z, Analysis of the Antioxidant Composition of Low Molecular Weight Metabolites from the Agarolytic Bacterium *Alteromonas macleodii* QZ9-9: Possibilities for High-Added Value Utilization of Macroalgae. *Antioxidants*, 11 (2022) 1977.

13 Razack SA, Suresh A, Sriram S, Ramakrishnan G, Sadanandham S, Veerasamy M, Nagalamadaka RB & Sahadevan R, Green synthesis of iron oxide nanoparticles using Hibiscus rosa-sinensis for fortifying wheat biscuits. *SN Appl Sci*, 2 (2020) 1.

14 Subramanian H, Krishnan M & Mahalingam A, Photocatalytic dye degradation and photoexcited anti-microbial activities of green zinc oxide nanoparticles synthesized *via Sargassum muticum* extracts. *RSC Adv*, 12 (2022) 985.

15 Muralidharan S & Vellaichamy A, Evaluation of anti-epithelial-mesenchymal transition property of *Garcinia mangostana* rind extract. *Future J Pharm Sci*, 7 (2021) 1.

16 El-Beltagi HS, Mohamed AA, Mohamed HI, Ramadan KM, Barqawi AA & Mansour AT, Phytochemical and potential properties of seaweeds and their recent applications: A review. *Mar Drugs*, 20 (2022) 342.

17 Nurshahida MF, Nazikussabah Z, Subramaniam S, Faizal WW & Aini MN, Physicochemical, physical characteristics and antioxidant activities of three edible red seaweeds (*Kappaphycus alvarezii, Eucheuma spinosum* and *Eucheuma striatum*) from Sabah, Malaysia. *IOP Conf Ser Mater Sci Eng*, 991 (2020) 012048.

18 Oladzadabbasabadi N, Ebadi S, Nafchi AM, Karim AA & Kiahosseini SR, Functional properties of dually modified sago starch/κ-carrageenan films: An alternative to gelatin in pharmaceutical capsules. *Carbohydr Polym*, 160 (2017) 43.

19 Fouda A, Eid AM, Abdelkareem A, Said HA, El-Belely EF, Alkhalifah DH, Alshallash KS & Hassan SE, Phyco-synthesized zinc oxide nanoparticles using marine macroalgae, Ulva fasciata Delile, characterization, antibacterial activity, photocatalysis, and tanning wastewater treatment. *Catal*, 12 (2022) 756.

20 Mansour AT, Alprol AE, Khedawy M, Abualnaja KM, Shalaby TA, Rayan G, Ramadan KM & Ashour M, Green synthesis of zinc oxide nanoparticles using red seaweed for the elimination of organic toxic dye from an aqueous solution. *Mater*, 15 (2022) 5169.

21 Ramesh AM, Pal K, Kodandaram A, Manjula BL, Ravishankar DK, Gowtham HG, Murali M, Rahdar A & Kyzas GZ, Antioxidant and photocatalytic properties of zinc oxide nanoparticles phyto-fabricated using the aqueous leaf extract of Sida acuta. *Green Process Synth*, 11 (2022) 857.

22 Bhuvaneshwari S, Padmalochana K, Savetha S & Natarajan A, Green Synthesis and Characterization Of Zinc Oxide Nanoparticles Using Seaweed Sulphated Polysaccharide and their Anti-Bacterial Properties. *Int J Eng Technol Manag Sci*, 4 (2022) 311.

23 Azizi S, Ahmad MB, Namvar F & Mohamad R, Green biosynthesis and characterization of zinc oxide nanoparticles using brown marine macroalga *Sargassum muticum* aqueous extract. *Mater Lett*, 116 (2014) 275.

24 Berneira LM, Poletti T, de Freitas SC, Maron GK, Carreno NL & de Pereira CM, Novel application of sub-Antarctic macroalgae as zinc oxide nanoparticles biosynthesizers. *Mater Lett*, 320 (2022) 132341.

25 Bashir M, Majid F, Bibi I, Mushtaq J, Ali A, Farhat LB, Katubi KM, Alwadai N, Khan MI & Iqbal M, Ultrasonic assisted synthesis of ZnO nanoflakes and photocatalytic activity evaluation for the degradation of methyl orange. *Arab J Chem*, 15 (2022)104194.

26 Yew YP, Shameli K, Miyake M, Kuwano N, Bt Ahmad Khairudin NB, Bt Mohamad SE & Lee KX, Green synthesis of magnetite (Fe_3O_4) nanoparticles using seaweed (*Kappaphycus alvarezii*) extract. *Nanoscale Reselett*, 11 (2016) 1.

27 Dinesh VP, Biji P, Ashok A, Dhara SK, Kamruddin M, Tyagi AK & Raj B, Plasmon-mediated, highly enhanced photocatalytic degradation of industrial textile dyes using hybrid ZnO@ Ag core–shell nanorods. *RSC Adv*, 4 (2014) 58930.

28 Sabry R, Fikry M, Ahmed OS, Zekri AR & Zedan AF, Laser-induced synthesis of pure zinc oxide nanoflakes. *J Phys Conf Ser*, 1472 (2020) 012005.

29 Nayem SA, Shah SS, Chaity SB, Biswas BK, Nahar B, Aziz MA & Hossain MZ, Jute stick extract assisted hydrothermal synthesis of zinc oxide nanoflakes and their enhanced photocatalytic and antibacterial efficacy. *Arab J Chem*, 15 (2022) 104265.

30 Wicaksono WP, Fadilla NI, Zamar AA, Fadillah G, Anugrahwati M, Anas AK & Kadja GT, Formaldehyde electrochemical sensor using graphite paste-modified green synthesized zinc oxide nanoparticles. *Inorg Chem Commun*, 143 (2022) 109729.

31 Anjali KP, Sangeetha BM, Raghunathan R, Devi G & Dutta S, Seaweed mediated fabrication of zinc oxide nanoparticles and their antibacterial, antifungal and anticancer applications. *Chem Select*, 6 (2021) 647.

32 Ebadi M, Zolfaghari MR, Aghaei SS, Zargar M, Shafiei M, Zahiri HS & Noghabi KA, A bio-inspired strategy for the synthesis of zinc oxide nanoparticles (ZnO NPs) using the

cell extract of *Cyanobacterium Nostoc* sp. EA03: from biological function to toxicity evaluation. *RSC adv*, 9 (2019) 23508.

33 Jiang S, Lin K & Cai M, ZnO nanomaterials: current advancements in antibacterial mechanisms and applications. *Front Chem*, 8 (2020) 580.

34 Vijayakumar S, González-Sánchez ZI, Malaikozhundan B, Saravanakumar K, Divya M, Vaseeharan B, Duran-Lara EF & Wang M, Biogenic synthesis of rod shaped ZnO nanoparticles using red paprika (*Capsicum annuum* L. var. *grossum* (L.) Sendt) and their *in vitro* evaluation. *J Clust Sci*, 32 (2021) 1129.

35 Kumar RV, Vinoth S, Baskar V, Arun M & Gurusaravanan P, Synthesis of zinc oxide nanoparticles mediated by Dictyota dichotoma endophytic fungi and its photocatalytic degradation of fast green dye and antibacterial applications. *S Afr J Bot*, 151 (2022) 337.

36 Khan AU, Ilyas M, Zamel D, Khan S, Ahmad A, Kaneez F, Abbas S, Armana S, Zaidi HU, Adnan F & Khan S, Bio-inspired fabrication of zinc oxide nanoparticles: Insight into biomedical applications. *Ann Adv Chem*, 6 (2022) 023.

37 Nhu VT, Dat ND, Tam LM & Phuong NH, Green synthesis of zinc oxide nanoparticles toward highly efficient photocatalysis and antibacterial application. *Beilstein J Nanotechnol*, 13 (2022) 1108.

38 Prabha M, Malviya T, Kumar A & Singh V, Effect of Gum acacia capped Cu-Ag bimetallic nanoparticles on ger mination and growth of gram seeds (*Cicer arietinum* L.). *Mater Today Proc*, 2023.

39 George BP, Rajendran NK, Houreld NN & Abrahamse H, Rubus capped zinc oxide nanoparticles induce apoptosis in MCF-7 breast cancer cells. *Mol,* 27 (2022) 6862.

40 Sadhukhan P, Kundu M, Chatterjee S, Ghosh N, Manna P, Das J & Sil PC, Targeted delivery of quercetin *via* pH-responsive zinc oxide nanoparticles for breast cancer therapy. *Mater Sci Eng C*, 100 (2019) 129.

41 Rani N & Saini K, Biogenic metal and metal oxides nanoparticles as anticancer agent: a review. *IOP Conf Ser Mater Sci Eng*, 1225 (2022) 012043.

42 Zadeh FA, Bokov DO, Salahdin OD, Abdelbasset WK, Jawad MA, Kadhim MM, Qasim MT, Kzar HH, Al-Gazally ME, Mustafa YF & Khatami M, Cytotoxicity evaluation of environmentally friendly synthesis Copper/Zinc bimetallic nanoparticles on MCF-7 cancer cells. *Rendi Lincei Sci Fis Nat*, 33 (2022) 441.

43 Anitha J, Selvakumar R, Hema S, Murugan K & Premkumar T, Facile green synthesis of nano-sized ZnO using leaf extract of *Morinda tinctoria*: MCF-7 cell cycle arrest, antiproliferation, and apoptosis studies. *J Ind Eng Chem*, 105 (2022) 520.